

Article

Study on Effects of Inlet Resistance on the Efficiency of Scroll Expander in Micro-Compressed Air Energy Storage System

Aiqin Sun ¹, Jidai Wang ^{1,*}, Guangqing Chen ^{1,*}, Jihong Wang ² , Shihong Miao ³, Dan Wang ³, Zhiwei Wang ¹ and Lan Ma ¹

¹ College of Mechanical and Electronic Engineering, Shandong University of Science and Technology, Qingdao 266590, China; saq80@sohu.com (A.S.); zwwang@live.com (Z.W.); 18853883050@163.com (L.M.)

² School of Engineering, University of Warwick, West Midlands, Coventry CV47AL, UK; jihong.wang@warwick.ac.uk

³ State Key Laboratory of Advanced Electromagnetic Engineering and Technology, School of Electrical and Electronic Engineering, Huazhong University of Science and Technology, Wuhan 430074, China; shmiao@hust.edu.cn (S.M.); wangdan@hust.edu.cn (D.W.)

* Correspondence: djdwang8911@sina.com (J.W.); chgq75@126.com (G.C.)

Received: 5 August 2020; Accepted: 1 September 2020; Published: 4 September 2020



Abstract: As an important part of a micro-compressed air energy storage system, the scroll expander directly affects the efficiency of the whole energy storage system. The effects of resistance on the efficiency of scroll expander caused by inlet structure and size are discussed with theory analysis and experimental methods in this paper. Micro-compressed air energy storage system has aroused widespread attention because of its pollution-free, high flexibility, in the community, remote areas power supply. Comprehensive experimental work with the selections of different size and structure of the air inlet of the scroll expander was performed with the cutting angle of air inlet chamber of the scroll expander. The results of the experiments are discussed on how exergy efficiency and inlet flow of the scroll expander were affected resulting from the cutting angles dissected. The results show that a maximum value exists for exergy efficiency of the scroll expander. Therefore, the exergy efficiency of the scroll expander can be effectively improved by enlarging the air inlet port dimension and modifying the size of air chamber.

Keywords: scroll expander; exergy efficiency; inlet resistance; experiment

1. Introduction

Compressed Air Energy Storage (CAES) plays an important role in balancing the load and generation of power grid through peak shaving, load shifting, and valley filling to encourage renewable energy source integration [1]. The key components of a compressed air energy storage system are usually an expander/turbine, gas storage tank, compressor, etc., which determine the energy conversion efficiency of the CAES system. It is important to improve those components' efficiency for the whole system efficiency improvement. In this paper, the efficiency analysis of an expander is considered. Different expanders are used in CAES systems, such as piston expander, turbo expander, and scroll expander [2,3], among which scroll expanders are widely valued in the micro-compressed air storage systems for the applications in transport, simple structure exhaust recovery, black starting torque generation due to their low gas pressure requirements, and smooth and continuous working performance [4].

From the current report, the research on scroll expanders is mainly focused on the applications of expanders in organic Rankine cycle systems, the profile equation, internal leakage, friction, etc. [5–12].

The study on how the inlet geometry changes affects the efficiency is hardly seen. To understand the influence of the inlet pressure and port size, it is necessary to conduct modeling and experimental study on the expanding process of a scroll expander [13]. The initial study was carried out through a prototype of scroll compression–expansion machine [14]. The authors of [14] found that the inlet structure (i.e., the rate of change of the inlet area) and the pressure loss of the scroll expander are the primary reason for change of energy conversion efficiency of the expander. Wu [15] confirmed that the structure of the air inlet is the main factor affecting energy conversion efficiency of the scroll expander. Compared with the circular air inlet hole, the opening characteristics of the waist-shaped air intake port can significantly improve the energy conversion efficiency.

To reduce the inlet resistance to air on the scroll expander, a mathematical model representing the relationship between the cutting angle of the head at the beginning of the intake chamber and the inlet size with the exergy efficiency is established in this paper. An experiment platform of compressed air energy storage system based on scroll expander is set up for accommodating this study. The influences of the inlet size and the cutting angle of the inlet chamber on the exergy efficiency of the scroll expander were tested with the new experimental platform.

2. Mathematical Model of a Scroll Expander

Scroll expander is a type of volumetric expander. The interior of the scroll expander is mainly composed of a pair of identical fixed and moving spirals with a phase difference mirrored with 180° . Several pairs of closed crescent-shaped work chambers are formed by the mutual engagement of two scrolls. A diagram of the geometric structure of a scroll-type inertial vortex rotor with no wall thickness is shown in Figure 1. The moving scroll is represented by the red line; the fixed scroll is represented by the blue line; and the orbit of the moving scroll is represented by dotted black line. Compressed gas enters the expander from the air inlet, which is in the center of the fixed scroll. The moving scroll is pushed to rotate. Gas volume increases, and pressure energy is converted into the mechanical energy of the expander spindle. In this paper, the scroll line of a scroll expander is discussed as circular involute, as shown in Figure 2.

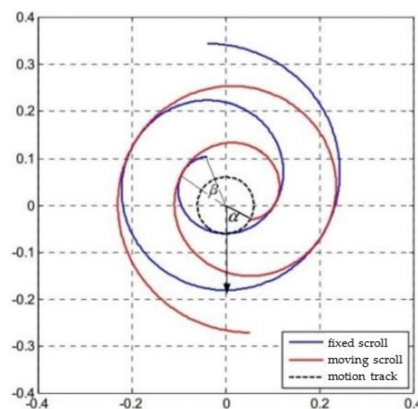


Figure 1. Geometry diagram of scroll expander.

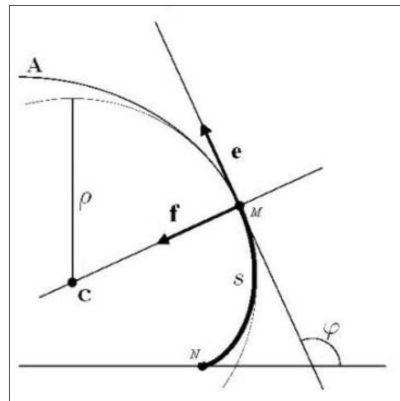


Figure 2. Circle involute curve.

2.1. Work Process Modeling of Scroll Expander

2.1.1. Geometric Modeling of Scroll Expander

In Figure 1, α indicates the angle between the head of the moving scroll and the negative direction of the y -axis, and the current position of the expander is represented by α . If the initial position of the moving scroll head is (x_0, y_0) , the moving scroll vortex curve equation is:

$$x_A(\varphi, \alpha) = x_0 + (\rho_0 + k\varphi) \sin \varphi + k \cos \varphi - k + r \sin \alpha \quad (1)$$

$$y_A(\varphi, \alpha) = y_0 - (\rho_0 + k\varphi) \cos \varphi + k \sin \varphi + \rho_0 - r \cos \alpha \quad (2)$$

where ρ_0 is the base radius of the involute curve, $\rho = \rho_0 + k\varphi$ is the radius of the involute curve, $k = d\rho/d\varphi$ determines the shape of the involute curve, φ is the unfolding angle of the moving scroll, $\varphi \in (\varphi, \varphi_{end})$, and φ_{end} is the tangential angle of the end of the moving scroll, as shown in Figure 2.

The fixed scroll vortex curve is:

$$x_B(\phi + j\pi) = x_0 + (\rho_0 + k(\phi + j\pi)) \sin(\phi + j\pi) + k \cos(\phi + j\pi) - k + r \sin(\phi + j\pi) \quad (3)$$

$$y_B(\phi + j\pi) = y_0 - (\rho_0 + k(\phi + j\pi)) \cos(\phi + j\pi) + k \sin(\phi + j\pi) + \rho_0 - r \cos(\phi + j\pi) \quad (4)$$

where ϕ is the unfolding angle of the involute curve of the fixed scroll, $\phi \in (\phi, \phi_{end})$, and ϕ_{end} is the tangential angle of the end of the fixed scroll.

As shown in Figure 1, it is specified that the center of the moving scroll orbit be the center for the convenience of representation. The angle between the line of original scroll head with the center and the line of position of the wall resection with center is defined as cutting angle at the beginning of the intake chamber, denoted by the symbol β . Assuming that the scroll tooth height is z , according to Green's formula [16], the intake chamber volume of scroll expander is:

$$V_c(\alpha) = \frac{1}{2}z \int_{\alpha+\beta}^{\alpha+\pi+\beta} -y_A(\varphi)d(x_A(\varphi)) + x_A(\varphi)d(y_A(\varphi)) + \frac{1}{2}z \int_{\alpha-\pi-\beta}^{\alpha-\beta} -y_B(\phi)d(x_B(\phi)) + x_B(\phi)d(y_B(\phi)) \quad (5)$$

Equations (1)–(4) are taken into Equation (5) to obtain:

$$V_c(\alpha) = \frac{z}{6} [\pi(2k^2(\pi^2 + 3\pi\beta + 3(\alpha^2 + \beta^2))) - 3k(\pi r - 2r\alpha + 2r\beta - 4\alpha\rho) + 3(r^2 + 2r\rho + 2\rho^2) - 6 \cos \beta (kr + (k - x_0)(-r + k(\pi + 2\beta)))(y_0 + \rho)(r + 2\rho) + k(-2x_0 + 2\alpha(y_0 + \rho)) \cos \alpha + 2(2k^2\alpha + k(r - (y_0 + x_0\alpha) - x_0(r + 2\rho)) \sin \alpha \sin \beta] \quad (6)$$

The range of expansion angle of the scroll wall profile of the first expansion chamber is $\varphi \in [\alpha + \beta + \pi, \alpha + \beta + 3\pi]$, $\phi \in [\alpha - \beta, \alpha - \beta + 2\pi]$, then the volume of the first expansion chamber is:

$$V_s(\alpha, i) = z\pi r[r + 2k(\pi + \alpha + \beta) + 2\rho - k \sin \beta] \quad (i = 1) \quad (7)$$

Similarly, the volume of the i th expansion chamber is:

$$V_s(\alpha, i) = z\pi r[r + 2k(\pi + 2(i-1)\pi + \alpha + \beta) + 2\rho - k \sin \beta] \quad (i = 1, 2, 3, 4 \dots n) \quad (8)$$

The exhaust chamber volume is:

$$V_e = V_{total} - V_c(\alpha) - \sum_{i=1}^n 2V_s(\alpha, i) \quad (9)$$

2.1.2. Thermodynamic Modeling of Scroll Expander

According to the literature [15], the thermodynamic parameters of each chamber of the scroll expander can be known.

The gas mass flow through the expander inlet is [17,18]:

$$\dot{m} = \frac{C_d C_0 A_s p_u f(p_r)}{\sqrt{T_u}} \quad (10)$$

where C_d is flow coefficient [19], A_s is the inlet cross-sectional area, T_u is the upstream temperature of the air inlet, p_u is the upstream gas pressure of the inlet, and $f(p_r)$ is as follows:

$$f(p_r) = \begin{cases} 1 & \frac{p_{atm}}{p_r} < p_r \leq C_r \\ C_k (p_r^{2/\gamma} - p_r^{(r+1)/\gamma})^{1/2} & C_r < p_r < 1 \end{cases} \quad (11)$$

where p_r is the ratio of the downstream to upstream gas pressure of the inlet. Assuming that the specific heat of air ratio $\gamma = 1.4$ and the gas constant is R ,

$$C_0 = \left[\frac{r}{R} \left(\frac{2}{\gamma+1} \right)^{\frac{\gamma+1}{\gamma-1}} \right]^{1/2} = 0.0404, \quad C_k = \left[\frac{2}{\gamma-1} \left(\frac{\gamma+1}{2} \right)^{\frac{\gamma+1}{\gamma-1}} \right]^{1/2} = 3.864, \quad C_r = \left(\frac{2}{\gamma+1} \right)^{\frac{\gamma}{\gamma-1}} = 0.528, \quad C_d = 0.61.$$

Finally, the thermodynamic model of intake process is obtained as follows:

$$\dot{T}_C = \frac{\frac{\dot{m}_1 h_1}{V_1} - \frac{\dot{V}_1}{V_1} [X_{air}] \bar{h} - [\dot{X}_{air}] \bar{h} + \frac{p_c [\dot{X}_{air}]}{[X_{air}]}}{[X_{air}] c_p - \frac{p_c}{T_c}} \quad (12)$$

$$\dot{p}_c = \frac{1}{V_c} \left(\frac{\dot{m}_c}{M_{air}} RT_c + \frac{m_c}{M_{air}} RT_c - p_c \dot{V}_c \right) \quad (13)$$

The expansion process model is:

$$\dot{T}_s = \frac{-\frac{\dot{V}_s}{V_s} [X_{air}] \bar{h}_s - [\dot{X}_{air}] \bar{h}_s + \frac{p_s [\dot{X}_{air}]}{[X_{air}]}}{[X_{air}] c_p - \frac{p_s}{T_s}} \quad (14)$$

$$\dot{p}_s = \frac{1}{V_s} \left(RT_s \frac{m_s}{M_{air}} - p_s \dot{V}_s \right) \quad (15)$$

The exhaust process model is:

$$\dot{T}_e = \frac{-\frac{\dot{m}_e h_e}{V_e} - \frac{\dot{V}_e}{V_e} [X_{air}] \bar{h}_e - [\dot{X}_{air}] \bar{h}_e + \frac{p_e [X_{air}]}{[X_{air}]}}{[X_{air}] c_p - \frac{p_e}{T_e}} \quad (16)$$

$$\dot{p}_e = \frac{1}{V_e} \left(\frac{\dot{m}_e}{M_{air}} RT_e + \frac{m_e}{M_{air}} RT_e - p_e \dot{V}_e \right) \quad (17)$$

where the subscripts c , s , and e represent the intake chamber, the expansion chamber, and the exhaust chamber, respectively. m is the gas quality, V is the chamber volume, X_{air} represents the gas molar volume concentration, M_{air} represents gas molar mass, \bar{h} is the gas molar heat capacity, and c_p is the specific heat capacity of the gas.

2.2. Exergy Efficiency Model of Scroll Expander

Exergy analysis not only considers the “quantity” of energy, but also combines the “quantity” and “quality” of energy. Compared with traditional energy analysis and entropy analysis, it reveals the transformation of “quantity” and “quality” in the process of energy transfer and conversion more profoundly.

Total driving torque of gas acting on moving scroll is [20]:

$$\tau_{total} = \sum_{i=1,2,\dots,n} z r p_s (\rho_i - \rho_{i+1}) (2\rho_0 + 2k\alpha + (4i + 1)k\pi) \quad (18)$$

where $\rho_i = p_i/p_s$ is the pressure ratio of the i th chamber pressure to the intake chamber pressure. The fluid motion parameters of various points in the internal flow field of the scroll expander are independent of time. Therefore, the gas flow in a scroll expander can be viewed as steady-state flow. The kinetic energy and position energy of the expander’s inlet and outlet are neglected, thus the exergy of the unit mass compressed air is [21]:

$$e_x = h - h_0 - T(S - S_0) \quad (19)$$

where h and h_0 represent the enthalpy of the unit mass compressed air and the enthalpy of the air in the ambient state, respectively. S and S_0 represent the entropy of the unit mass compressed air and the entropy of the air in the ambient state.

Assume that the heat capacity is c_p , the pressure of the compressed air is p , the temperature is T , the ambient temperature is T_0 , the atmospheric pressure is p_0 , and gas constant is R_g . If air is considered as the ideal gas, then:

$$h - h_0 = \int_{T_0}^T c_p dT \quad (20)$$

$$S - S_0 = \int_{T_0}^T \frac{c_p}{T} dT - R_g \ln \frac{p}{p_0} \quad (21)$$

Combining Equations (20) and (21) into Equation (19), the exergy of unit mass compressed air can be expressed as:

$$e_x = \int_{T_0}^T c_p dT - T_0 \left(\int_{T_0}^T \frac{c_p}{T} dT - R_g \ln \frac{p}{p_0} \right) = c_p (T - T_0) - T_0 \left(c_p \ln \frac{T}{T_0} - R_g \ln \frac{p}{p_0} \right) \quad (22)$$

Then exergy efficiency of scroll expander can be calculated by:

$$\eta_{ex} = \frac{W_{sh}}{\dot{m}_1 e_{x1} - \dot{m}_2 e_{x2}} = \frac{\tau \omega / 9550}{\dot{m}_1 e_{x1} - \dot{m}_2 e_{x2}} \quad (23)$$

where $c_p = 1.004 \text{ kJ}/(\text{kg}\cdot\text{k})$, $p_0 = 0.1 \text{ MPa}$, and $T_0 = 303 \text{ K}$. e_{x1} and e_{x2} are, respectively, the exergy of the inlet gas and the exhaust gas, which can be calculated by Equation (22). \dot{m}_1 and \dot{m}_2 represent the intake flow and the exhaust flow, which can be calculated by Equation (10).

To sum up, by substituting the geometric volume equation, thermodynamic equation, and kinetic equation of the scroll expander into the exergy efficiency equation of the expander, the relationship between the chamber volume and exergy efficiency can be obtained, and it can be seen that the cutting angle of the intake chamber and the size of the air inlet will affect the efficiency of the scroll expander.

3. Study on Experimental Performance of Scroll Expander

The above modeling shows that the exergy efficiency of the scroll expander for compressed air energy storage is related to inlet size and cutting angle. The compressed gas with a certain pressure enters into the intake chamber of the scroll expander through the inlet, which causes the throttle loss to a certain extent due to the throttle obstruction of the inlet and restricts the increase of the compressed gas flow rate. The existence of the head at the beginning of the intake chamber of the vortex disc has a certain blocking effect on the flow of compressed gas into the expander, which reduces the pressure energy used to drive the spindle of the expander to rotate. To further study the effect of the inlet size and the cutting angle on the efficiency of the expander, the following experiments were carried out.

3.1. Introduction of Experiment System

The scroll expander selected for this experiment was modified from the ATC-086 scroll compressor. The original compressor outlet valve was removed. The main structural parameters are shown in Table 1. The main equipment of the experiment platform includes air compressor, air tank, scroll expander, and magnetic powder brake. Measuring instruments are pressure regulator, temperature sensors, pressure sensors, flow sensors, torque and speed sensors, and data acquisition system.

Table 1. The main structural parameters of the scroll expander.

Name	Symbol	Value	Name	Symbol	Value
Base circle radius/mm	ρ_0	3.3	Number of scroll turns	N	2.35
Involute initial angle/rad	α	0.71	Base circle center distance/mm	r	5.45
Involute pitch/mm	P	20.7	Original inlet diameter/mm	-	8
Scroll height/mm	z	33.5	Outlet diameter/mm	-	15

The instrument and equipment parameters are shown in Tables 2 and 3. The experiment platform for the compressed air energy storage system is shown in Figure 3. Air compressor, gas tank, scroll expander, and magnetic powder brake were connected one after the other to form the main body of the compressed air energy storage system. The working medium of the experiment platform was compressed air, which was produced by a low-pressure compressor and stored in the gas tank to reach the set pressure for the expander to do work.

In the energy release stage, the compressed air with a certain pressure enters the scroll expander to do work after being adjusted to a certain value through the pressure reducing valve. Compressed air enters the expander to expand, pushing the spindle to do work. The pressure sensor, flow sensor, and temperature sensor set in front of the expander measure the state parameters of the compressed air in the inlet of the expander. The torque and speed sensors collect the torque and speed of spindle. The magnetic powder brake at the end of the system, as the load of the system, converts the mechanical work transferred by the spindle into heat energy to consume the work generated by the expander. The compressed air is discharged from the exhaust outlet of the scroll expander. The sensor placed at the exhaust port of the expander measures the flow, pressure, and temperature of the discharged gas. Then, the exergy efficiency is calculated by substituting the measured inlet and outlet gas

parameters into the formula derived above. During the experiment, the collection and preservation of all parameters were completed by data acquisition system dSPACE.

Table 2. The main equipment parameters.

Name	Parameter/Model
Air compressor	LH15-0.85/35
Gas tank	Design pressure 1.05 MPa, Volume 1000 L
Scroll expander	ATC-086-03
Magnetic brake	FZ-25J/Y

Table 3. Test instruments.

Name	Model	Range	Accuracy
Temperature sensor	CWDZ11-HK-04-V4-19-L50-G	-50–50 °C	±0.5 °C
Pressure sensor	SDE1-D10-G2-W18-L-PU-M8	0–10 bar	±0.2 bar
Flow sensor	SFAM-62-5000L-M-2SV-M12	50–5000 L/min	±(3% o.m.v. + 0.3% FS)
Torque and speed sensor	JN338A	Torque 20 N·m Speed 6000 rpm	0.2% FS

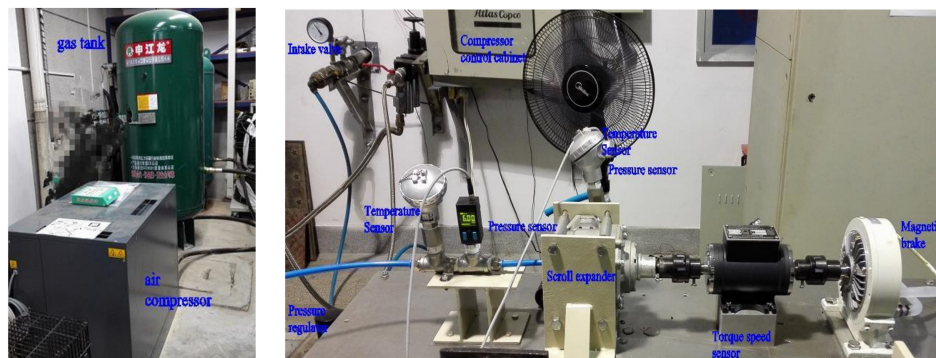


Figure 3. Experimental platform of compressed air energy storage system.

3.2. Analysis of Experiment Data

3.2.1. Research on Air Inlet Size of Scroll Expander

The air inlet opened in the fixed scroll baseplate is the only channel for compressed air to enter the expander. Air inlet size directly affects the amount of throttling loss of compressed air. To reduce the intake resistance, the influence of the size of the inlet of the scroll expander on its exergy efficiency was researched. The air inlet located at the center of the fixed scroll baseplate is expanded to different sizes. To ensure that the air inlet is not communicated with the chambers other than the air intake chamber, the maximum opening range of the air inlet is tangent to the beginning of the wrap, which is 14 mm, as shown in Figure 4.

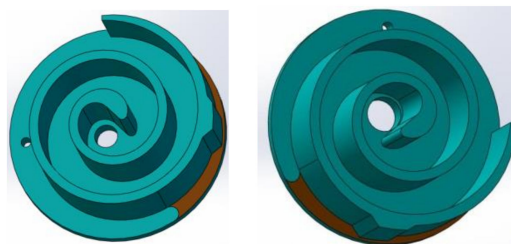


Figure 4. Maximum opening range of air inlet.

The original inlet diameter of the expander is 8 mm. Therefore, the inlet size of the expander is taken as 8, 10, 12, and 14 mm. The experiments were conducted separately. The effects of the inlet port size on the performance of scroll expander are shown in Figure 5. Figure 5a shows that, when the inlet pressure is 0.27 MPa, the exergy efficiency of the scroll expander is the highest. With the increasing of the intake pressure, the exergy efficiency gradually decreases, and the decreasing rate gradually decreases. When the inlet pressure is kept constant, the exergy efficiency of the scroll expander gradually increases as the inlet expands. When the inlet diameter of the scroll expander is expanded from 8 to 14 mm, the overall exergy efficiency of the scroll expander is increased by about 2%. Therefore, the exergy efficiency of the scroll expander can be improved effectively by expansion of the inlet size, especially when the intake pressure is below 0.3 MPa. When the inlet pressure is 0.27 MPa, the exergy efficiency can be increased by about 6%. When the inlet pressure is greater than 0.3 MPa, the effect of the inlet port size on the exergy efficiency of the expander is poor, only ranging from 1% to 2%. This is because of the limited expansion of the inlet port size. For the higher pressure, the smaller change in the size of the air intake has less effect on the intake air volume.

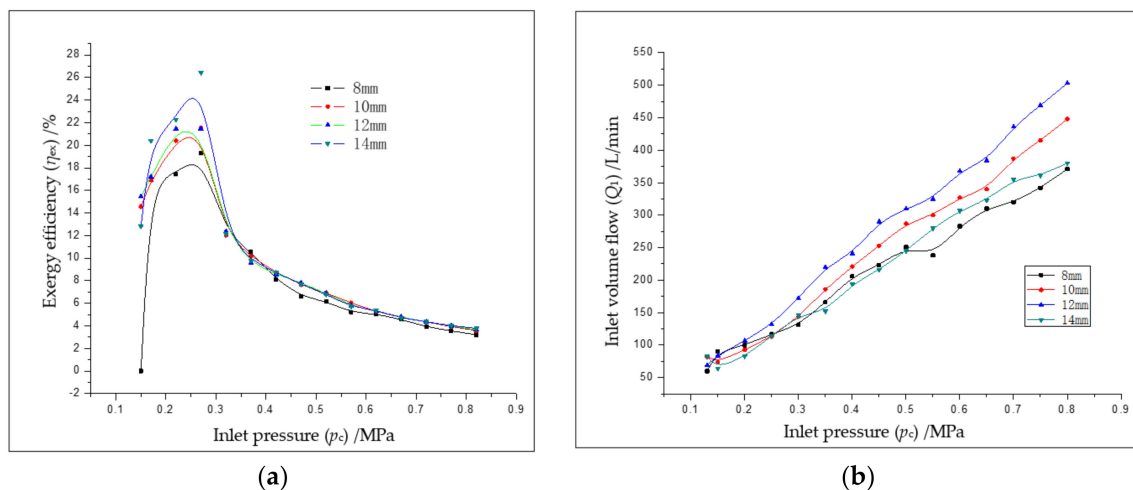


Figure 5. Influence of air inlet size on the performance of the expander: (a) influence of inlet size on exergy efficiency; and (b) influence of inlet size on inlet flow.

In Figure 5b, with the increase of the air inlet, the air flow of the scroll expander generally increases. As the inlet pressure increases, the rate of increase continues to increase. When the inlet pressure is 0.8 MPa, the inlet flow of the expander increases by 33.3% compared with the original expander. This is mainly due to the expansion of the air inlet, so that the inlet resistance of the expander is reduced, the throttling loss is reduced, and the gas flow into the interior of the expander is increased. It can also be seen that the exergy efficiency is not a single value function of the inlet size.

These results indicate that the exergy efficiency of the scroll expander can be improved effectively by increasing size of the air inlet port. Therefore, the size of the inlet can be increased while ensuring it has no connection with the expansion chamber.

3.2.2. Research on Cutting Angle of Inlet Chamber of Scroll Expander

To research the influence of the intake chamber wall on the exergy efficiency of the scroll expander, the cutting angle of the intake chamber head of the scroll wall is, respectively, 45° , 90° , 135° ... 360° resection, as shown in Figure 6. Some processed objects are shown in Figure 7.

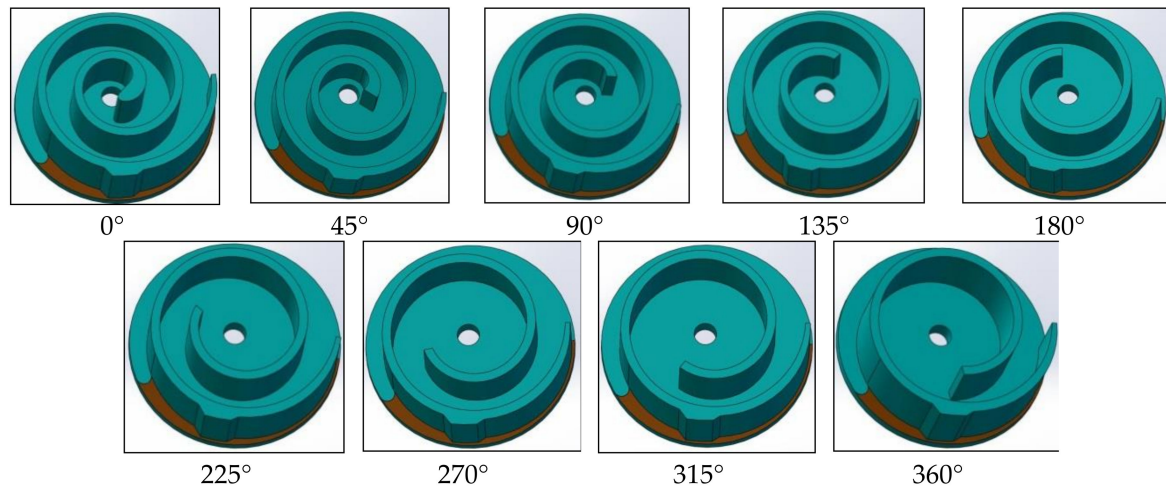


Figure 6. Different cutting angle diagrams of intake chamber wall.



Figure 7. Cutting photos of intake chamber.

The effects of the cutting angle of the scroll in the intake chamber on the exergy efficiency at different inlet pressures are shown in Figure 8, where, according to the effect of the air inlet size on exergy efficiency, the air inlet port size in the experiment is 14 mm. Figure 8a shows that the cutting angle has less effect on the exergy efficiency with the increase of the inlet pressure. When the inlet pressure is 0.28 MPa, the maximum exergy efficiency of the scroll expander is increased by about 8% at the angle of 180°. When the inlet pressure is greater than 0.3 MPa, the exergy efficiency of the scroll expander decreases significantly with the increase of the inlet pressure, which is reduced from an increase of 8% to about 2%. This shows that the influence of the 180° resection of the intake chamber head on the expansion exergy efficiency of the expander is more effective at the low pressure. When the intake pressure is between 0.3 and 0.4 MPa, the highest efficiency point of the expander is caused by 315° cutting the head, the exergy efficiency of the expander is increased by about 12.5%, and the corresponding intake pressure is 0.32 MPa. This is caused by two reasons: (1) the same expander is used in this group of experiments, and after several times of dismantling and processing the leak of the expander is increased; and (2) the contact area at the wall end of the movable and fixed scroll is reduced, and the internal leakage is increased for the removal of the wall head of the intake chamber. When the inlet pressure is greater than 0.4 MPa, it can be clearly observed that the improvement rate of the exergy efficiency is greatly reduced, and the minimum increase is about 2%. Within this range of intake pressure, the most improvement of the exergy efficiency of the turbo-expander is caused by the 225° angle of the wall head resection, which is increased by about 10%.

As shown in Figure 8b, with the increase of the cutting angle of the intake chamber head, the inlet flow of the expander increases continuously. When the inlet chamber is cut 180° and the inlet air pressure of the expander is 0.2 MPa, the inlet flow of the expander increases by 35%. When the inlet chamber is cut 315° and the inlet air pressure of the expander is 0.3–0.4 MPa, the inlet flow is increased by 50%. When the inlet chamber is cut 225° and the inlet air pressure of the expander is greater than 0.4 MPa, the inlet flow of the expander increases by 30.3%.

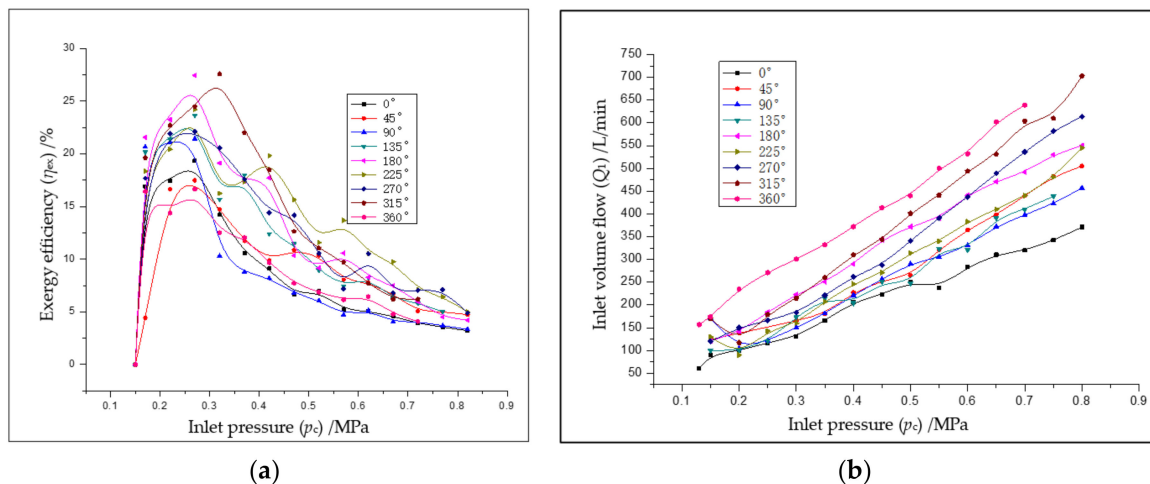


Figure 8. Effect of the cutting angle on the work performance: (a) effect of cutting angle on exergy efficiency; and (b) effect of cutting angle on inlet flow.

4. Conclusions

The following conclusions can be drawn from the experiments on the influence of different inlet sizes and different cutting angles of the intake chamber wall on the exergy efficiency of the scroll expander:

- (1) The exergy efficiency of the scroll expander can be effectively increased by increasing the size of the air inlet, up to 6%. Therefore, the air inlet of the expander can be opened as large as possible and the air inlet is not communicated with other chambers than the air intake chamber.
- (2) Increasing the exergy efficiency of the expander can be achieved by proper resection of the intake chamber of the scroll expander. Under different inlet pressures, the best head cutting angles of intake chamber wall are different: when the inlet pressure of the expander is 0.2–0.3 MPa, the cutting angle is 180°, with the exergy efficiency of the scroll expander increased by up to 8%; when the inlet pressure is 0.3–0.4 MPa, the cutting angle is 315°, with the exergy efficiency of the expander increased by 12.5%; and when the inlet pressure is greater than 0.4 MPa, the cutting angle is 225°, which increases the exergy efficiency of the scroll expander by about 10%.

Author Contributions: All authors contributed to this work in collaboration. J.W. (Jidai Wang), A.S. and J.W. (Jihong Wang) conceived and designed the experiments. G.C. and L.M. performed the experiments. All the authors contributed to the discussion and data analysis. S.M. and D.W. contributed experimental platform. Z.W. contributed analysis tools. J.W. (Jidai Wang) and A.S. wrote the paper. All authors have read and agreed to the published version of the manuscript.

Funding: This work was supported by China National Basic Research Program 973 (2015CB251301) and Open Fund of Huazhong University of Science and Technology State Key Laboratory of Advanced Electromagnetic Engineering and Technology (2017KF004).

Conflicts of Interest: The authors declare no conflict of interest.

Nomenclature

ω_m	Rotor speed of scroll expander and PMSG (rad/s)
J_{system}	The whole micro CAES system Inertias (kg/m^2)
$K_{S-GS}(\omega_m)$	Combined effect on torque from static and Coulomb frictions of scroll expander and generator
K_f	The coefficient of the viscous frictions of the scroll expander and PMSG
τ	Scroll expander effective driving torque (Nm)
τ_e	Electromagnetic torque of the PMSG (Nm)
ω_e	Electromagnetic angular velocity of PMSG (rad/s)
p_n	Number of the pole pairs of the PMSG
T	Air temperature (K)

p	Air pressure (Pa)
V	Volume (m^3)
z	Height of the scroll wall (m)
k	Slope of the curvature radius
r	Radius of the orbit (m)
α	Orbit angle of the moving scroll (rad)
ρ	Radius of the curvature (m)
ρ_0	Initial radius of the curvature for moving scroll curve (m)
R	Ideal gas constant ($\text{J}\cdot\text{K}^{-1}\text{kg}^{-1}$)
m	Mass of the air (kg)
C_V	Special heat of the air per mole at the temperature ($\text{kJ}\cdot\text{K}^{-1}\cdot\text{m}^3$)
j	Numbers of the scroll wraps
\dot{m}	Mass flow rate of the air (kg/s)
X_s	Effective open area of the orifice (m^2)
C_d	Discharge coefficient
C_0	$C_0 = 0.04(\sqrt{\text{kJ}/\text{kg}})$
C_k	$C_k = 3.864$
p_u	Upstream pressure of the orifice (Pa)
p_d	Downstream pressure of the orifice (Pa)
p_r	The ratio between the downstream p_d and upstream p_u
u	Voltage in the different axes for the PMSG modeling (V)
i	Current in the different axes for the PMSG modeling (A)
ψ_f	Magnetic flux of the PMSG (Wb)
L_d, L_q	Inductances of d axis and q axis, respectively (H)
R_e	Resistance of the PMSG stator windings (ohm)
P_e	The power consumed by the electrical load (W)
P_{air}	The employed air power by the expander (W)
h	The special enthalpy of air (J/kg)
η	The discharging process energy efficiency
η_{e+cold}	The overall discharging process energy efficiency considering of refrigerating
P_{cold}	The cold air power supplied by the expander (W)

Subscripts

C, S	The scroll expander's center and side chambers, respectively
d, q	The d, q axes for the PMSG modeling
in, out	The inlet and outlet of scroll expander

Abbreviations

CAES	Compressed air energy storage
PHS	Pumped hydroelectric storage
PMSG	Permanent magnet synchronous

References

1. Wang, J.D.; Lu, K.; Ma, L.; Wang, J.; Dooner, M.; Miao, S.; Li, J.; Wang, D. Overview of compressed air energy storage and technology development. *Energies* **2017**, *10*, 991. [[CrossRef](#)]
2. Li, X. Study on the Influence of Component Characteristics for Advanced Adiabatic Compressed Air Energy Storage System. Ph.D. Thesis, University of Chinese Academy of Sciences (Institute of Engineering Thermophysics), Beijing, China, 2015.
3. Zhang, X. Multistage Radial Turbine for Supercritical Compressed Air Energy Storage System. Ph.D. Thesis, University of Chinese Academy of Sciences (Institute of Engineering Thermophysics), Beijing, China, 2014.
4. Lemofouet, S.; Rufer, A. A hybrid energy storage system based on compressed air and supercapacitors with maximum efficiency point tracking. *IEEE Trans. Ind. Electron.* **2006**, *53*, 1105–1115. [[CrossRef](#)]
5. Huang, Y.; Yu, Y. The choice of refrigerants in a rankine-rankine cycle refrigeration system using scroll expander. *Fluid Mach.* **1997**, *25*, 52–55.

6. Saitoh, T.; Yamada, N.; Wakashima, S.I. Solar rankine cycle system using scroll expander. *J. Environ. Eng.* **2007**, *2*, 708–719. [[CrossRef](#)]
7. Wang, J.; Luo, X.; Yang, L.; Mangan, S.; Derby, J.W. Mathematical modeling study of scroll air motors and energy efficiency analysis-part I. *IEEE/ASME Trans. Mechatron.* **2011**, *16*, 122–132. [[CrossRef](#)]
8. Yang, L.; Wang, J.; Ke, J. Development of a mathematical model for a scroll type air motor. *Polym. Eng. Sci.* **2006**, *28*, 321–332.
9. Yang, L.; Wang, J.; Mangan, S.; Derby, J.W.; Lu, N. Mathematical model and energy efficiency analysis of a Scroll-type air motor. *IAENG Int. J. Appl. Math.* **2008**, *38*, 14–19.
10. Mendoza, L.; Lemoufouet, S.; Schiffmann, J. Testing and modelling of a novel oil-free co-rotating scroll machine with water injection. *Appl. Energy* **2017**, *185*, 201–213. [[CrossRef](#)]
11. Li, L.; Ao, L.; Shen, L.; Hu, Y. Improvement and experimental research on the performance of scroll expander using organic Rankine cycle (ORC). *Chem. Ind. Eng. Prog.* **2017**, *36*, 1642–1648.
12. Luo, X.; Wang, J.; Sun, H. A novel magnetic scroll expander as a drive for electricity generation. *IET Digit. Libr.* **2014**, 1–6. [[CrossRef](#)]
13. Yang, X.; Pan, J.; Wang, J.; Sun, J. Simulation and experimental research on energy conversion efficiency of scroll expander for micro-compressed air energy storage system. *Int. J. Energy Res.* **2014**, *38*, 884–895.
14. Yang, X. Performance Study of Scroll Compressor/Expander Composite Machine in Compressed Air Energy Storage. Ph.D. Thesis, East China University of Science and Technology, Shanghai, China, 2014.
15. Wu, Z.; Yan, J.; Xie, F.; Zhu, T.; Gao, N. Research on the effect of suction port shape on a scroll expander pressure loss during the suction process. *Compress. Technol.* **2016**, 1–6. [[CrossRef](#)]
16. Department of Mathematics of Tongji University. *Advanced Mathematics*, 7th ed.; Higher Education Press: Beijing, China, 2014; p. 204.
17. Harris, E. Compressed air theory and computations. *Astrophys. J. Suppl.* **2007**, *120*, 587–599.
18. Wang, J.; Pu, J.; Moore, P. A practical control strategy for servo-pneumatic actuator systems. *Control Eng. Pract.* **1999**, *7*, 1483–1488. [[CrossRef](#)]
19. Huang, W.; Li, J.; Xiao, Z. *Engineering Fluid Mechanics*; Chemical Industry Press: Beijing, China, 2009; p. 281.
20. Li, L. *Scroll Compressor*; Machinery Industry Press: Beijing, China, 1998; p. 85.
21. Fu, Q. *Thermodynamic Analysis Methods of Energy Systems*; Xi'an Jiaotong University Press: Xi'an, China, 2005; p. 104.



© 2020 by the authors. Licensee MDPI, Basel, Switzerland. This article is an open access article distributed under the terms and conditions of the Creative Commons Attribution (CC BY) license (<http://creativecommons.org/licenses/by/4.0/>).